



1

Deriving Cropland N₂O Emissions from Space-Based NO₂ Observations

Taylor J. Adams¹, Genevieve Plant¹, Eric A. Kort¹

¹Department of Climate and Space Sciences and Engineering, University of Michigan, Ann Arbor, MI, USA

5 *Correspondence to:* Taylor Adams (adamsta@umich.edu) &/or Eric Kort (eakort@umich.edu)

Abstract: Croplands are the largest anthropogenic source of nitrous oxide (N₂O), a potent greenhouse gas and ozone-depleting substance. Agricultural emissions produce small atmospheric signals with high spatiotemporal variability presenting a large observational challenge. If capable, space-based observations could characterize cropland N₂O emissions from farmlands across the world. No current satellite can resolve near-surface N₂O variations from cropland emissions. However, satellite observations of nitrogen dioxide (NO₂), a component of NO_x along with nitric oxide (NO), capture cropland emissions. NO, which quickly converts to NO₂ in the atmosphere, and N₂O are co-emitted from soils. Both gases are produced by microbial soil processes, and are emitted in large amounts as a result of excess nitrogen from applied fertilizer. Given their co-emission in croplands, we ask: Can satellite NO₂ observations be used to infer N₂O emissions? We examine coincident airborne N₂O and NO₂ measurements downwind of California croplands to characterize N₂O:NO_x emission relationships from farms. We use these emission ratios to transform estimates of agricultural NO_x emissions derived from space-based TROPOMI NO₂ observations to N₂O emissions. We compare these estimates to independent ground and airborne studies in the US Corn Belt and Mississippi River Valley. Space-based estimates are broadly consistent with these ground and airborne studies, suggesting that satellite NO₂ observations can be used to infer cropland N₂O emissions. Further refinement of a NO₂ proxy approach for cropland N₂O emissions has the potential to expand observational capabilities to constrain regional and global cropland N₂O emissions and inform process models.

1 Introduction:

Nitrous oxide (N₂O) is a potent greenhouse gas and ozone-depleting substance with sizable anthropogenic emissions. In a 100-year time frame, N₂O has a global warming potential 298 times that of carbon dioxide (Butterbach-Bahl et al., 2013; Ravishankara et al., 2009). With a long atmospheric lifetime (over 100 years) and no tropospheric sink, N₂O emitted from the surface travels to the stratosphere where it can react with excited oxygen atoms to produce reactive nitrogen oxide radicals that deplete stratospheric ozone. N₂O is now the largest contributor to stratospheric ozone depletion of actively emitted anthropogenic gases (Ravishankara et al., 2009). Since the 1700's the atmospheric concentration of N₂O has increased by over 60 parts per billion (ppb) (Tian et al., 2024), with an accelerating rate in recent years (Liang et al., 2022).

Agriculture is a dominant source of N₂O emissions, contributing 3.8 (2.5-5.8) Tg N₂O-N per year, or about 22% (15%-34%) of global emissions, from 2007 to 2016, with a 30% increase over the past four decades due to nitrogen fertilization (Tian et al., 2020). This trend is expected to accelerate due to the growing demand for food and resources that support agricultural industries as well as waste and industrial processes, highlighting the urgent need for mitigation efforts (Davidson and Kanter, 2014).

Much of what we know about agricultural N₂O emissions is the result of near-surface N₂O measurements from soil flux chambers. Observations from chamber systems range from ~10 samples per day (automatic chambers) (Rowlings et al., 2015; Sihi et al., 2020) to as infrequently as daily or monthly scales (manual chambers) (Griffis et al., 2013). The small spatial extent of chamber measurements, along with the availability of coincident auxiliary data (e.g., soil moisture, N application rates), permits robust mechanistic analyses of soil N₂O emissions. However, given the spatial heterogeneity of N₂O emissions (Lawrence et al., 2021), the small spatial resolution (~1m²) of chamber measurements becomes a limitation when assessing emissions at larger spatial scales. Eddy covariance methods can be used to study N₂O emissions at the field scale, with sensitivity to surface emissions from upwind soils of ~10 to



1000 m² (di Marco et al., 2005). Observational constraints at much larger scales are possible with tall (~100's of meters in height) tower measurements of N₂O, which are interpreted with atmospheric transport and inverse modeling to infer N₂O emissions. This provides emissions information integrated over several hundred kilometers at a monthly temporal resolution (Chen et al., 2016; Griffis et al., 2013; Nevison et al., 2018, 2023).

More recently, airborne sampling approaches have demonstrated the potential to bridge the scale gap from flux chambers/eddy-flux to tall-towers. Depending on their flight altitude, airborne measurements can resolve N₂O emissions at the farm (~1-2 km) scale (Gvakharia et al., 2020) while sampling an area of several hundred kilometers (Dacic et al., 2024; Desjardins et al., 2015; Eckl et al., 2021; Gvakharia et al., 2020; Herrera et al., 2021; Jimenez et al., 2005; Kort et al., 2008; Xiang et al., 2013). The limitation of airborne observations is that they capture short time windows and sample targeted regions as part of campaigns such as CalNex (2010) (Xiang et al., 2013), FEAST (2017) (Gvakharia et al., 2020) and MAIZE (2021 & 2022) (Dacic et al., 2024; Kort et al., 2022, 2024a, 2024b).

Current observational methods to constrain N₂O emissions for the study of process-level emission controls or mitigation strategies are currently limited to the targeted ground and airborne approaches detailed above. A remote-sensing, space-based solution would have the potential to assess agricultural N₂O emissions at key spatiotemporal scales and broaden the spatial extent of studies beyond those limited by targeted ground and airborne measurements. However, presently, we cannot directly measure surface-level N₂O signals from cropland emissions with a space-based platform. A promising opportunity, however, lies in the widespread remote sensing of nitrogen dioxide (NO₂). Nitric oxide (NO) is co-emitted with N₂O from agricultural soils (Davidson et al., 2000), and the NO is largely oxidized to NO₂ within seconds to minutes after emission (Jacob, 1999). Given that N₂O and NO are co-emitted and their emission patterns are driven by similar variables (e.g., fertilizer application) (Harrison et al., 1995; Sanhueza et al., 1990), variability in atmospheric NO₂ concentrations from agricultural soils may serve as a useful proxy for corresponding N₂O emissions. Space-based NO₂ observations, available globally almost daily from TROPOMI, track spatiotemporal variations in NO₂ in both urban (Adams et al., 2023; Goldberg et al., 2019a, b, 2021, 2024; Ialongo et al., 2020; Park et al., 2022) and agricultural (Ghude et al., 2010; Huber et al., 2020, 2024; Lin et al., 2023) areas, and have done so for decades (Gonzalez Abad et al., 2019). Beyond the existence of NO₂ instrumentation in space, the relatively short lifetime of NO₂ means emissions of NO₂ lead to large enhancements concentrated in the boundary layer, providing a large signal to observe. For N₂O, in contrast, emissions add only a very small enhancement over large background values (often less than 1ppb signals on background over 330ppb, Dacic et al., 2024), which creates a larger observational challenge.

In this work, we explore the potential of using space-based NO₂ observations as a proxy for agricultural N₂O emissions. We first discuss the driving mechanisms for N₂O and NO (NO₂) from managed croplands. We then use coincident airborne observations of NO₂ and N₂O from the California Research at the Nexus of Air Quality and Climate Change (CalNex) campaign conducted in California in 2010 to derive N₂O-to-NO_x emission ratios for large spatial regions commensurate with satellite remote sensing of NO₂. The aircraft sampling captures integrated emissions ratios that include heterogeneity of emissions in response to a number of driving process-level variables. We hypothesize that we can apply the observed emission ratio distribution to NO_x emissions derived from satellite NO₂ observations to obtain an estimate of N₂O emissions from space-based observations. This then enables observational analyses that cover large regions of the world and can track changes over time. We evaluate this possibility for the corn belt and the Mississippi River Valley in the USA.

2 Emissions of N₂O and NO from Managed Croplands

N₂O and NO emissions in agricultural soils result from the microbial processes of nitrification and denitrification, with N₂O predominating during denitrification (Baggs, 2008; Chen et al., 1995; Müller et al., 2003) and NO during nitrification (Skiba et al., 1993). Soil moisture influences these processes, where high water-filled pore space (WFPS) favors denitrification and low WFPS favors nitrification. This moisture dependency contributes to large emissions of N₂O and NO following rainfall events (Kim et al., 2012; Scholes et al., 1997), and poorly drained soils are known to emit more N₂O than well-drained soils, which is an important management consideration for N₂O



3

90 reduction strategies (Lawrence et al., 2021). Drier soils favor higher NO:N₂O emission ratios, often close to or greater than unity, whereas wet soils can have emission ratios closer to 0 (~0.1) (Anderson and Levine, 1987; Davidson, 1992; Johansson and Sanhueza, 1988; Lipschultz et al., 1981; Tortoso and Hutchinson, 1990). Crop type also influences the NO:N₂O ratio (Anderson and Levine, 1987).

95 Fertilizer application is the most important common driver of NO and N₂O emissions, and fertilized soils have higher missions of both trace gases (Harrison et al., 1995; Liu et al., 2017; Sanhueza et al., 1990; Shepherd et al., 1991). The accumulation of fertilizer is also hypothesized to drive large post-rainfall emissions of N₂O (Cardenas et al., 1993; Johansson, 1984; Johansson and Sanhueza, 1988; Levine et al., 1996) NO_x (NO + NO₂) (Ghude et al., 2010; Jaeglé et al., 2004; Oikawa et al., 2015; Scholes et al., 1997; Smith et al., 1997).

100 Given the link between fertilizer application and enhancements of NO and N₂O, we hypothesize that spatiotemporal patterns in NO_x emissions from croplands may be a useful proxy to estimate agricultural N₂O emissions. Over extended spatial and temporal scales that incorporate a variety of soil conditions and crop types, the variability in NO:N₂O emissions should be reduced compared to shorter, more localized observations, such as those made in chamber studies. This integrating effect may increase the fidelity of using emissions ratios to derive N₂O emissions.

3 Deriving Emission Ratios from CalNex Airborne N₂O and NO₂ Observations

105 Satellite observations of NO₂ from TROPOMI or TEMPO, with ground pixel sizes in the range of 5.5x3.5 - 2x4.75 km, will be sensitive to the integrated emissions that emerge from entire farms and multi-farm conglomerates and counties (~250 km² (Merlos and Hijmans, 2020). To characterize the cropland emission behavior at comparable spatial scales, we use airborne sampling of N₂O and NO₂ to determine an emissions relationship between these gases downwind of agricultural fields. Very few airborne campaigns have been made with continuous, high-accuracy, 110 high-precision measurements of N₂O and NO₂ in agricultural regions. For the analysis here we use observations from one of the few campaigns that collected such measurements, the CalNex campaign in 2010 (Fig. 1A), which sampled the San Joaquin and Sacramento Valleys during 6 flights between May 7 and June 18, 2010 (Data available at: <https://csl.noaa.gov/projects/calnex/>). In-flight instrumentation included the Harvard/National Center for Atmospheric Research's (NCAR) Dual Quantum Cascade Laser Spectrometer for measurement of N₂O (Jimenez et al., 2005; Kort et al., 2011), and a chemiluminescence NO₂ sensor (Pollack et al., 2010; Ryerson et al., 1999, 2001, 115 2003). During CalNex, measurements of these gases were reported at a 1s rate, and we applied an additional 5-second centered rolling average to reduce instrument noise. To isolate cropland regions, analysis is restricted to locations >0.04° (~3.7 – 4.4 km) from regions with emissions in the top 1% of the National Emissions Inventory (NEI) (Strum et al., 2017), and to periods when the aircraft was below 500m elevation.

120 Literature often reports NO:N₂O molecular ratios from chamber studies. In this work we determine N₂O:NO_x molecular ratios from the aircraft as this is the factor we apply to satellite-derived NO_x emissions to generate N₂O emissions. Since our observations are not made in near proximity to the soil, we assume all the emitted soil NO_x (primarily NO) has converted in the atmosphere to NO₂, consistent with previous studies (Huber et al., 2020; Jacob, 1999). The inverse of our ratios is directly comparable to literature NO:N₂O molecular emissions ratios.

125 We apply two methods to characterize N₂O:NO_x emission relationships from the CalNex airborne dataset. Figure 1B and 1C show histograms of derived emission or enhancement ratios corresponding to each approach overlaid over flight maps with the location of data from those approaches. We use these emission or enhancement ratios to characterize the heterogeneity in the empirical relationship between N₂O and NO_x at the farm to multi-farm scale. Below, we briefly outline each approach.



4

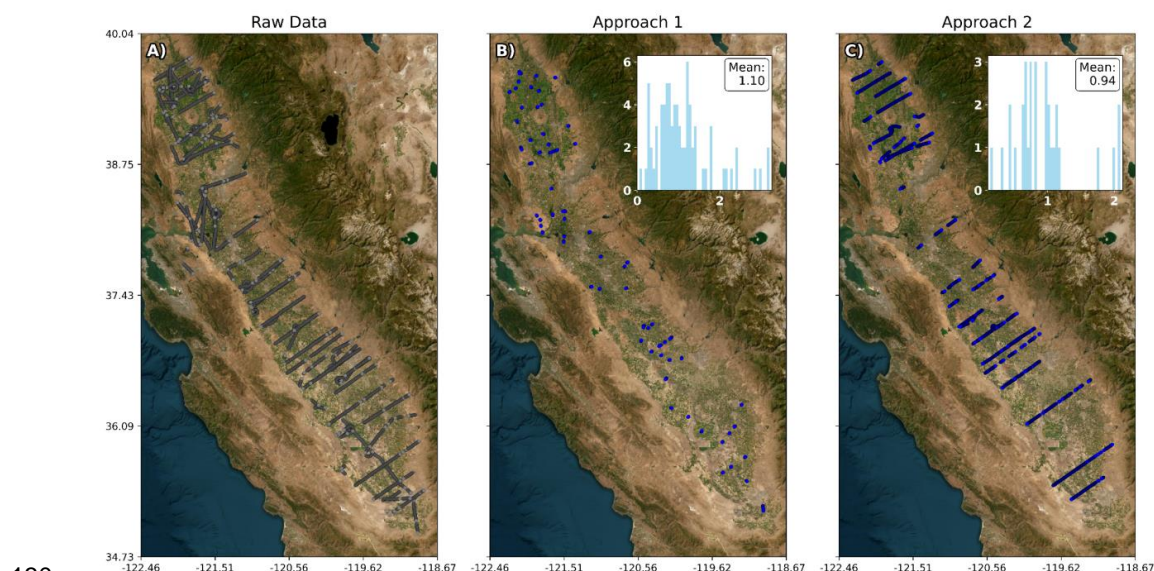


Figure 1: Flight maps corresponding to data remaining after filtering steps in A) the raw CalNex dataset filtered for data within the agricultural field and away from high NO₂-emission areas, B) in approach 1 and C) in approach 2. A histogram showing the distribution of molecular emission ratios determined in each respective approach is overlaid upon the map. Satellite imagery credit: Esri.

Approach 1 seeks to isolate signals from cropland emissions within ~10 km of the aircraft to determine N₂O:NO_x emission relationships. We isolate enhancements from these nearby emissions by filtering for distinct peaks in N₂O concentration and accounting for the chemical loss of NO₂. A similar method has been performed to isolate plumes from nearby natural gas flares in the Bakken (Gvakharia et al., 2017). First, we determine N₂O and NO₂ enhancements as the concentration above the 5th percentile of a rolling, centered, one-minute window for every data point. We then isolate cases that are separated by at least 5 seconds in time (~500+ meters in space) where N₂O is enhanced and both NO₂ and N₂O's perturbations exceed instrument noise. We require 8 or more observations where the range from minimum to maximum N₂O concentration enhancement exceeds 0.09 ppb, corresponding to greater than 2σ (0.064 ppb) uncertainty in the mean (based on instrument precision of 0.09 ppb). Cases are removed if their slopes are below zero, as these do not imply co-emission. The distribution of N₂O:NO_x emission ratios post-filtering cases is shown in Fig. 1B.

We account for photochemical loss of NO₂ by estimating the distance from the source to the observed N₂O enhancement. Assuming the width of an observed enhancement represents a plume's width, we estimate the transport distance from the plume's origin using rural dispersion parameters from Zannetti et al., (2013). We assume a moderately unstable atmosphere during CalNex. Based on daily wind conditions, we estimate the transport time relative to the average NO₂ lifetime and adjust NO₂ accordingly to approximate the quantity of emitted NO_x. We then derive a N₂O:NO_x emission ratio using type-II ranged major axis regression of the isolated N₂O and NO₂ concentration enhancements.

The average chemistry corrected enhancement emission ratio (referred to as the emission ratio from here forward) is 1.10 ppb N₂O / ppb NO_x, a slightly lower value than the ratio (1.22 ppb N₂O / ppb NO_x) if chemical loss is not accounted for. This adjustment is small compared to the variance we see in the ratio. The final dataset using this approach results in 78 individual plumes observed in the nearfield of croplands to derive N₂O:NO_x, as shown in Fig. 1B. This approach is designed to isolate enhancements specific to aggregated cropland sources, and the resultant



molecular emissions ratio distribution will encompass variation due to a number of variable drivers of emissions in the upwind region (crop type, fertilizer, soil moisture, etc...).

160 *Approach 2* incorporates data at broader spatial scales. With this method, we isolate individual flight legs, or portions of the aircraft transects, that are perpendicular to daily wind direction and downwind of agricultural fields. We then treat each flight leg's $\text{N}_2\text{O}:\text{NO}_x$ relationship as a unique enhancement ratio, deriving the background as we do in *approach 1* and assuming impacts from chemical loss are averaged out across flight legs. We do not correct for the chemical loss of NO_2 , or filter for distinct peaks in N_2O concentration to isolate near-field emissions in this approach. This approach, rather than isolating small-scale cropland emissions as in approach 1, derives the enhancement relationship across the cropland. This provides significantly more observations but derives an enhancement ratio. To determine the emissions ratio, we then assume chemistry or other processes contribute negligibly, in which case the emissions ratio is equivalent to the enhancement ratio. Approach 2 yields an average molecular emissions ratio of 0.94, determined using type-II ranged major axis regression on the N_2O and NO_2 concentration enhancements. Flight legs considered in this method can be visualized in Fig. 1C.

As seen in Fig. 1, we obtain similar mean $\text{N}_2\text{O}:\text{NO}_x$ ratios from each method, demonstrating that the relationship is robust to methodological differences and assumptions. The distributions of the derived $\text{N}_2\text{O}:\text{NO}_x$ values for each approach are also comparable. The Kruskal-Wallis test performed between these two distributions yields a p-value of 0.9983, suggesting no significant difference in median or distribution, and the Welch's t-test, compared between them, shows there is no significant difference between the emission ratios. Emission ratios range between 0.06 and 3.20 ppb N_2O / ppb NO_x (0.3125 - 16.6 ppb $\text{NO}_x:\text{N}_2\text{O}$) for approach #1 and 0.14 and 2.09 ppb N_2O / ppb NO_x (0.48 - 7.14 ppb $\text{NO}_x:\text{N}_2\text{O}$) for approach #2, reflecting the expected heterogeneity in $\text{N}_2\text{O}:\text{NO}_x$ ratio over agricultural lands, and demonstrating that increasing the spatial scale aggregated to create these ratios dampens variability. These values we observe are in line with literature from soil-chamber measurements which report heterogeneous $\text{NO}_x:\text{N}_2\text{O}$ emission ratios ranging from near 0 to as high 7 (Johansson and Sanhueza, 1988) in tropical savannahs, or even 10 to 20 in fully aerobic environments (Tortoso and Hutchinson, 1990). This variation occurs as a function of factors such as fertilizer application, crop-type, and other management and environmental factors (Anderson and Levine, 1987; Davidson, 1992; Johansson and Sanhueza, 1988; Lipschultz et al., 1981). As expected with the larger spatial scale of our airborne approach, integrating over variable soil conditions and crop types, our ratios show less variability than prior soil chamber studies and decrease in variability as more observations are aggregated. In the following sections, we use emission ratios derived from approach #2, though there is little sensitivity to this choice.

4 Deriving N_2O from Satellite NO_2 Observations:

With $\text{N}_2\text{O}:\text{NO}_x$ emissions ratios derived from the aircraft measurements, N_2O emissions can be determined from space if soil NO_x emissions are calculated from space-based NO_2 observations. Many different methods could be applied to derive NO_x emissions estimates from satellite NO_2 observations. For instance, Huber et al., (2020) applied a box model to estimate NO_x emissions from TROPOMI-observed NO_2 enhancements within the Mississippi River Valley, Ghude et al., (2010) inferred top-down NO_x emissions from OMI by mass balance, and Lin et al., (2023) estimated soil NO_x emissions in TROPOMI grid cells based on seasonal variation. In principle, the emissions ratios derived in Sect. 3 can be used to estimate agricultural N_2O emissions from space-based observations of NO_2 . Here, we use a simple chemical box model and TROPOMI NO_2 observations to demonstrate quantification of agricultural N_2O using space-based NO_2 observations as a proxy. We focus our analysis on three regions (Figure 2) in the USA where independent ground and airborne measurement campaigns have previously been conducted to determine N_2O emissions, providing a bases for direct comparison with this new approach. This is a robust challenge for this method, as the emissions ratios are determined from aircraft data collected over California in 2010, and crop-type, management practice, soil moisture, and other driving variables can be quite different in these central US regions.

In this work, we use TROPOMI Version 02.04.00 (S5P_L2_NO2_HiR_2) NO_2 retrievals (KNMI). TROPOMI observations are filtered for a quality assurance value greater than or equal to 0.75, indicating high-quality data per the operational retrieval (Van Geffen et al., 2020). We use these TROPOMI NO_2 observations in a chemical box



6

model to determine agricultural NO_x emissions for the Mississippi River Valley, Nebraska, and Iowa, employing a similar data-model approach as previously outlined in Huber et al., (2020). The chemical box model defined by equation 1:

$$E_{soil,NO_2} = \frac{U\Delta(NO_{2,VCD})}{X} + \frac{V\Delta(NO_{2,VCD})}{Y} + \frac{V_d(NO_{2,VCD})}{Z_{PBL}} + \frac{NO_{2,VCD}}{t} - E_{NEI}, \quad (1)$$

The first two terms in Eq. 1 captures advection, representing NO₂ advected into and out of a domain of interest. Here, U represents the average zonal wind speed (m/s) across the box of interest and X is the distance of the east-to-west edge of the domain of interest. $\Delta(NO_{2,VCD})$ is the mean TROPOMI NO₂ column enhancement (molecule/m²) above the background abundance, which we define as the 5th percentile of NO₂ abundance in the domain of interest. V to denote the meridional winds and Y to denote the north-to-south edge distance along the domain of interest. The third term denotes deposition, where V_d denotes the deposition velocity (m/s) from Yang et al., (2010) (Deposition velocity by month: DJF, 0.02 cm/s; MAM, 0.16 cm/s; JJA, 0.29 cm/s; SON, 0.06 cm/s). NO_{2,VCD} is the average NO₂ vertical column density in the domain of interest and Z_{PBL} is the boundary layer height estimate over the domain of interest. Similar to Huber et al., (2020), Z_{PBL} is set to 1000m over the course of the study. The fourth term represents chemical loss, where NO_{2,VCD} again denotes the NO₂ vertical column density in the domain of interest and “t” represents the lifetime of NO_x. The final term E_{NEI} denotes the average fossil fuel NO_x emissions in the domain of interest from the 2014 NEI inventory (Strum et al., 2017), averaged monthly to eliminate noise.

In this work, we analyze TROPOMI NO₂ retrievals on a daily scale. The size and location of the analysis domain vary depending upon the region of interest but are at minimum comparable to the size of the box model used in (Huber et al., 2020) (0.75 x 0.75 degree). We additionally exclude TROPOMI overpasses from the study if they incorporate less than 30 TROPOMI NO₂ observations in our box model domain. Once NO_x emissions are derived using Equation 1 we multiply soil NO_x emissions (E_{soil,NO_x} units of nmole/m²/sec), by the aircraft-derived N₂O:NO_x molecular emission ratio to obtain an estimate of N₂O flux, E_{soil,N_2O} , units of nmole/m²/sec (Equation 2).

$$E_{soil,N_2O} = (ER_{N_2O:NO_x})E_{soil,NO_x}, \quad (2)$$

To incorporate the impact of variability in the observationally derived emission ratio on estimated N₂O emissions in this analysis, we employ a Monte Carlo approach where we propagate variation in the N₂O:NO_x emission ratio through to N₂O emissions. We iterate through the daily average values of TROPOMI-derived NO_x emissions and multiply each by all emission ratios shown in Fig. 1C to derive all possible N₂O emissions from the variation in N₂O:NO_x. We then randomly sample one of these N₂O realizations over 10,000 iterations to create a distribution of TROPOMI NO₂-derived N₂O emissions. The 2.5th percentile and the 97.5th percentile define the 95% confidence interval, with the mean providing a central estimate.

5 Comparison with Independent Estimates of N₂O

We compare the space-based N₂O emissions estimates with N₂O emissions from independent studies. We first compare N₂O emissions derived from TROPOMI-NO₂ observations with those obtained from chamber measurements reported by Lawrence et al., (2021). The chamber measurements, conducted between February 2017 and October 2019 in Iowa crop fields, are compared only for the warm season (May-September) of 2018 and 2019 when TROPOMI was operational, and chamber data was available. The comparison domain spans -94.055 to -93.305 in latitude (0.75 degrees) and 41.605 to 42.355 in longitude (0.75 degrees). The domain of interest lies to the north of Des Moines, Iowa, and is centered on the Ames, Iowa field site referenced in Lawrence et al., (2021)(41.98°N, 93.68°W), and is shown in Fig. 2A, with a star indicating the chamber location.



7

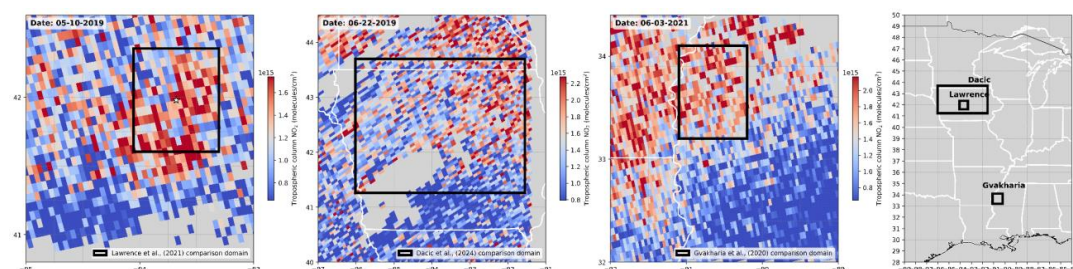


Figure 2: TROPOMI tropospheric NO₂ columns and the box model domains used for comparison with A) Lawrence et al., 2021 with a star denoting the chamber location, B) Dacic et al., 2024, and C) Gvakharia et al., 2020. D) Each corresponding region shown on a map of the central US.

We calculate the confidence interval for the Lawrence et al., (2021) chamber dataset by randomly sampling daily average values on days that we also have TROPOMI NO₂-derived N₂O estimates and calculating a 95th confidence interval. For the same observational time-window, we derive daily N₂O emission estimates for the domain of interest using the proxy-method described in Sect. 4. The distribution of chamber-N₂O emissions and its associated 95% confidence interval against the mean and 95% confidence interval for TROPOMI NO₂-derived N₂O flux are shown in Fig. 3A.

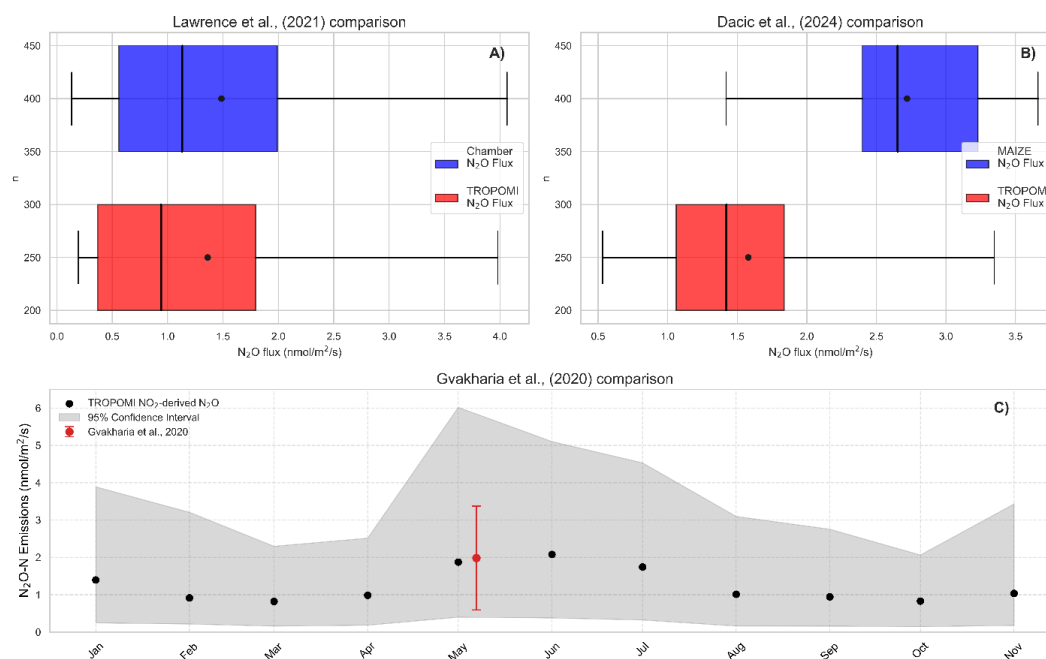


Figure 3: Satellite derived estimates concurrence with independent studies. (A, top left) Box plots of the distribution of daily average N₂O flux derived from chamber observations detailed in Lawrence et al., 2021 and TROPOMI observations from that period. (B, top right) Box plots of N₂O flux observed by TROPOMI across the MAIZE campaign domain, and ensemble averages for coincident days of the MAIZE (2021-2022) campaign. (C, Bottom) TROPOMI-NO₂ derived N₂O flux (gray distribution) compared against the N₂O flux estimate from Gvakharia et al., (2020) (red band).

The confidence interval for the mean chamber-derived N₂O flux largely overlaps with that of the TROPOMI NO₂-derived N₂O flux (Fig. 3A). The mean values differ by ~8.7%, with the chamber-derived flux averaging 1.36 (0.561),



5.22; 95% CI) $\text{nmol N}_2\text{O}/\text{m}^2/\text{s}$ and the TROPOMI-derived flux averaging 1.49 (0.16, 4.54; 95% CI) $\text{nmol N}_2\text{O}/\text{m}^2/\text{s}$. We evaluate the difference in these means with a nonparametric permutation test, which indicated the observed differences between population means were not significantly different. These are independent dataset and methods that operate on different scales. The relative agreement in mean values and the overlap in confidence intervals suggest that the TROPOMI-based approach provides a reasonable estimate of long-term chamber-derived mean N_2O flux in this study.

Next, we compare TROPOMI NO_2 -derived N_2O fluxes with N_2O emissions derived from aircraft observations during the Measurements of Agriculture Illuminating farm-Zone Emissions of N_2O (MAIZE) 2021 and 2022 campaigns (Dacic et al., 2024; Kort et al., 2022, 2024a, 2024b). These airborne campaigns measured N_2O concentrations over the Iowa croplands during May and June of both years. Observed N_2O concentrations were linked to the surface using an atmospheric transport model, and an ensemble of surface fluxes was derived using a Bayesian inversion framework. In this comparison, we use a larger analysis domain to match the area over which the MAIZE campaigns took place. For 5 flight days of the MAIZE campaign (2021-05-31, 2021-06-03, 2022-05-18, 2022-05-20, and 2022-05-21), we produce a TROPOMI NO_2 -derived N_2O average flux for the MAIZE domain (S: 40.398; N: 43.399; W: -96.724; E: -90.044, Fig. 2B). We compare this with MAIZE daily ensemble averages. We then randomly sample using the previously described Monte Carlo resampling approach to obtain a 95% confidence interval for MAIZE N_2O flux. Figure 3B shows the comparison between airborne-informed MAIZE N_2O flux and N_2O flux we derive from TROPOMI NO_2 observations and our aircraft-derived emission ratios.

While the mean TROPOMI-derived N_2O flux is within the 95% confidence interval of the MAIZE emissions, and vice versa (Fig 3B), there is less notable agreement than in the comparison with the chamber emissions from Lawrence et al., (2021) for a similar domain. There exist multiple possible reasons for the larger apparent discrepancy. 1) The comparison is limited to only five days. 2) The MAIZE aircraft flights captured a heavy-tail emissions distribution with small number of fields contributing substantially to total emissions. These high emissions events might be missed by chamber observations, and the coarse scale of the satellite observations used here might reduce sensitivity to small regions with high emissions, thus explaining the TROPOMI and chamber relative agreement with both values lower than determined by flights in MAIZE. 3) It is also possible the enhancement ratio approach used here is failing to capture the emissions ratio as well as desired for this place and time. Still, the mean emissions rate determined from satellite is captured within the airborne campaign 95% confidence interval, and thus it appears this space-based proxy approach can provide a reasonable mean estimate for this region with five days of observations.

Finally, we compare N_2O fluxes derived using the proposed space-based NO_2 proxy method to fluxes derived from airborne mass balance estimates from Gvakharia et al., (2020) over the Mississippi River Valley. During the Fertilizer Emissions Airborne Study (FEAST) in Spring 2017, Gvakharia et al., (2020) observed N_2O fluxes of $1.98 \pm 1.39 \text{ nmol N}_2\text{O-N}/\text{m}^2/\text{s}$ in May 2017, noting significant spatial variation. The TROPOMI instrument was not operational until late 2018, so we do not have overlapping data to directly compare TROPOMI NO_2 -derived N_2O flux estimates with those from Gvakharia et al., (2020). Instead, we calculate emissions for a full calendar year for 2021 and compare these estimates with the May 2017 estimate from the FEAST data (see Fig. 2C and 3C). With the space-based proxy approach, we observe seasonal variation ranging from $0.82 \text{ nmol N}_2\text{O-N}/\text{m}^2/\text{s}$ in March to a peak of $2.1 \text{ nmol N}_2\text{O-N}/\text{m}^2/\text{s}$ in June, and our spring estimate is in close agreement with the estimate from Gvakharia et al., (2020) is shown in Fig. 3C. Specifically, we estimate $1.89 \text{ nmol N}_2\text{O-N}/\text{m}^2/\text{s}$ in May (5.6% difference) using TROPOMI NO_2 observations from 2021.

We find the TROPOMI NO_2 -derived N_2O flux compares favorably with various independent measures of N_2O flux and emissions from the corn belt (Dacic et al., 2024; Lawrence et al., 2021) and Mississippi River Valley (Gvakharia et al., 2020). For two of the comparison, space-based estimates are within ~10% of these independently obtained N_2O estimates, despite this testing capturing multiple regions and time-periods, and the airborne derived emission ratios coming from observations in a completely different agricultural region. This agreement demonstrates the potential of scaling satellite-based NO_2 observations with $\text{N}_2\text{O}:\text{NO}_x$ emission ratios to capture agricultural N_2O



emissions, and that such an approach may provide a viable method to estimate N₂O emissions from agricultural regions around the world.

310 6 Conclusion:

Constraining global emissions of N₂O is crucial to understanding its spatiotemporal emission distribution, drivers of emissions, and to guide effective mitigation strategies. Ground-based measurements are inherently limited to the regions where they are installed, while airborne methods are often limited to targeted, short-duration research campaigns. North America has been the focus of many studies, but less is known about the other large agricultural regions around the world. Satellite observations, thus, are an attractive option because they have the potential for more spatial coverage (~global during the warm season) and relatively fine (~daily) temporal resolution. This can also serve to bridge the gap that exists between the present point- and region-scale N₂O monitoring. In the absence of direct space-based observations of surface N₂O concentrations, we propose to leverage the well-observed trace gas NO₂ as a proxy for N₂O emissions to create a pathway to monitor N₂O emissions in global agricultural regions more comprehensively.

In this work, we derive airborne N₂O-to-NO_x emission ratios from the CalNex (2010) airborne campaign around a dense agricultural region of California. These ratios represent the molecular emissions ratio of N₂O to NO_x from croplands at spatial scales commensurate with space-based NO₂ observations. We combine these ratios with satellite-derived NO_x soil emissions to estimate N₂O emissions. We compare our TROPOMI NO₂-derived N₂O fluxes with N₂O emissions estimates from independent chamber observations and two distinct airborne campaigns made in Iowa and the Mississippi River Valley. Our space-based N₂O emissions estimates compare favorably with these independent estimates across different regions and as measured by different methods covering different spatial and temporal scales. In comparison with chamber-derived N₂O flux (Lawrence et al., 2021), our estimate of mean flux only differs by 8.7%, or ~0.13 nmol N₂O/m²/s. Mean estimates differ from airborne emission ratios taken in the Mississippi River Valley (Gvakharia et al., 2020) by ~5.6%. Comparing emissions derived from Bayesian inversion of aircraft data (Dacic et al., 2024) yields a larger N₂O flux mean difference by ~50%. In all cases, the confidence intervals of our space-based N₂O flux estimates and those from independent measurements and approaches overlap.

In this work, we demonstrate that space-based NO₂ observations as a proxy for N₂O cropland emissions compare favorably to independent estimates across multiple agricultural areas and years. This suggests that space-based NO₂ retrievals are a viable and robust proxy for N₂O flux at scales of at least 0.75 x 0.75 degrees, and over timescales as short as five days. Further development and refinement of approaches to characterize agricultural NO₂ from satellite observations and link them to N₂O emissions are possible. As presented here, the largest source of uncertainty in the estimated N₂O emissions derives from the large variability in the observed airborne N₂O:NO_x emissions ratio. Improved understanding and definition of this ratio, and what controls variation, could improve the fidelity of this proxy approach. Nonetheless, this work has demonstrated a proxy-based approach that may offer a path towards a more spatially comprehensive constraint on regional and global budgets of agricultural N₂O emissions.

Code Availability

Data Availability

All data used in this manuscript are archived in public databases. Airborne data from P3 aircraft during the CalNex campaign is available from the NOAA Chemical Sciences Laboratory at <https://csl.noaa.gov/projects/calnex/>. TROPOMI Level 2 Nitrogen Dioxide total column products, Version 02, are available from the European Space Agency at <https://doi.org/10.5270/S5P-9bnp8q8>. The National Emission Inventory is available from the Environmental Protection Agency at <https://www.epa.gov/air-emissions-inventories/2017-national-emissions-inventory-nei-data>. Chamber flux measurements from Lawrence et al. (2021) are available at <https://doi.org/10.6073/pasta/e6117972f6a80d5f5a9db354957910ed>. Airborne data from the FEAST campaign and Gvakharia et al. (2020) is available at <https://doi.org/10.7302/Z2XK8CRG>. Posterior fluxes from the airborne MAIZE campaign and Dacic et al. (2024) are available at <https://doi.org/10.7302/9w5m-mn30>.



Author Contribution

TA developed the box model code, conducted all model simulations, and designed and optimized the aircraft data filtering methods. TA also prepared the manuscript, with significant input from EK and GP. EK conceived the project idea. EK and GP provided guidance on methodology and the presentation of results, and contributed to data collection and modeling for the experimental datasets used for comparison.

Competing Interest

Acknowledgements

The authors acknowledge the University of Michigan for supporting this work. The authors thank Dr. Daniel Huber and Dr. Natasha Dacic for their assistance with running the box model and interpreting the MAIZE results respectively. The authors also thank the CalNex, FEAST, MAIZE and TROPOMI science teams for their high-quality data collection and sharing of data into public archives.

Financial Support

References:

- Adams, T. J., Geddes, J. A., and Lind, E. S.: New Insights Into the Role of Atmospheric Transport and Mixing on Column and Surface Concentrations of NO₂ at a Coastal Urban Site, *Journal of Geophysical Research: Atmospheres*, 128, e2022JD038237, <https://doi.org/10.1029/2022JD038237>, 2023.
- Anderson, I. C. and Levine, J. S.: Simultaneous field measurements of biogenic emissions of nitric oxide and nitrous oxide., *J Geophys Res*, 92, 965–976, <https://doi.org/10.1029/JD092ID01P00965>, 1987.
- Baggs, E. M.: A review of stable isotope techniques for N₂O source partitioning in soils: recent progress, remaining challenges and future considerations, *Rapid Communications in Mass Spectrometry*, 22, 1664–1672, <https://doi.org/10.1002/RCM.3456>, 2008.
- Butterbach-Bahl, K., Baggs, E. M., Dannenmann, M., Kiese, R., and Zechmeister-Boltenstern, S.: Nitrous oxide emissions from soils: How well do we understand the processes and their controls, *Philosophical Transactions of the Royal Society B: Biological Sciences*, 368, <https://doi.org/10.1098/RSTB.2013.0122>, 2013.
- Cardenas, L., Rondon, A., Johansson, C., and Sanhueza, E.: Effects of soil moisture, temperature, and inorganic nitrogen on nitric oxide emissions from acidic tropical savannah soils, *J Geophys Res*, 98, 14783–14790, <https://doi.org/10.1029/93JD01020>, 1993.
- Chen, Y., Tessier, S., MacKenzie, A. F., and Laverdière, M. R.: Nitrous oxide emission from an agricultural soil subjected to different freeze-thaw cycles, *Agric Ecosyst Environ*, 55, 123–128, [https://doi.org/10.1016/0167-8809\(95\)00611-U](https://doi.org/10.1016/0167-8809(95)00611-U), 1995.
- Chen, Z., Griffis, T. J., Millet, D. B., Wood, J. D., Lee, X., Baker, J. M., Xiao, K., Turner, P. A., Chen, M., Zobitz, J., and Wells, K. C.: Partitioning N₂O emissions within the U.S. Corn Belt using an inverse modeling approach, *Global Biogeochem Cycles*, 30, 1192–1205, <https://doi.org/10.1002/2015GB005313>, 2016.
- Copernicus Sentinel data processed by ESA, Koninklijk Nederlands Meteorologisch Instituut (KNMI), Sentinel-5P TROPOMI Tropospheric NO₂ 1-Orbit L2 5.5km x 3.5km, Greenbelt, MD, USA, Goddard Earth Sciences Data and Information Services Center (GES DISC), Accessed 2025/09/04, [10.5270/S5P-9bnp8q8](https://doi.org/10.5270/S5P-9bnp8q8), 2021
- Dacic, N., Plant, G., and Kort, E. A.: Airborne Measurements Reveal High Spatiotemporal Variation and the Heavy-Tail Characteristic of Nitrous Oxide Emissions in Iowa, *Journal of Geophysical Research: Atmospheres*, 129, e2024JD041403, <https://doi.org/10.1029/2024JD041403>, 2024.
- Davidson, E. A.: Sources of Nitric Oxide and Nitrous Oxide following Wetting of Dry Soil, *Soil Science Society of America Journal*, 56, 95–102, <https://doi.org/10.2136/SSSAJ1992.03615995005600010015X>, 1992.



- 395 Davidson, E. A. and Kanter, D.: Inventories and scenarios of nitrous oxide emissions, *Environmental Research Letters*, 9, 105012, <https://doi.org/10.1088/1748-9326/9/10/105012>, 2014.
Davidson, E. A., Keller, M., Erickson, H. E., Verchot, L. V., and Veldkamp, E.: Testing a Conceptual Model of Soil Emissions of Nitrous and Nitric Oxides: Using two functions based on soil nitrogen availability and soil water content, the hole-in-the-pipe model characterizes a large fraction of the observed variation of nitric oxide and nitrous
400 oxide emissions from soils, *Bioscience*, 50, 667–680, [https://doi.org/10.1641/0006-3568\(2000\)050\[0667:TACMOS\]2.0.CO;2](https://doi.org/10.1641/0006-3568(2000)050[0667:TACMOS]2.0.CO;2), 2000.
Desjardins, R., Rochette, P., Pattey, E., and MacPherson, I.: Measurements of greenhouse gas fluxes using aircraft- and tower-based techniques, *Agricultural Ecosystem Effects on Trace Gases and Global Climate Change*, 45–62, <https://doi.org/10.2134/ASASPECPUB55.C3>, 2015.
- 405 Eckl, M., Roiger, A., Kostinek, J., Fiehn, A., Huntrieser, H., Knote, C., Barkley, Z. R., Ogle, S. M., Baier, B. C., Sweeney, C., and Davis, K. J.: Quantifying Nitrous Oxide Emissions in the U.S. Midwest: A Top-Down Study Using High Resolution Airborne In-Situ Observations, *Geophys Res Lett*, 48, e2020GL091266, <https://doi.org/10.1029/2020GL091266>, 2021.
Van Geffen, J., Folkert Boersma, K., Eskes, H., Sneep, M., Ter Linden, M., Zara, M., and Pepijn Veefkind, J.: S5P TROPOMI NO₂ slant column retrieval: Method, stability, uncertainties and comparisons with OMI, *Atmos Meas Tech*, 13, 1315–1335, <https://doi.org/10.5194/AMT-13-1315-2020>, 2020.
- 410 Ghude, S. D., Lal, D. M., Beig, G., Van Der A, R., and Sable, D.: Rain-induced soil NO_x emission from India during the onset of the summer monsoon: A satellite perspective, *Journal of Geophysical Research Atmospheres*, 115, 16304, <https://doi.org/10.1029/2009JD013367>, 2010.
- 415 Goldberg, D. L., Lu, Z., Streets, D. G., De Foy, B., Griffin, D., McLinden, C. A., Lamsal, L. N., Krotkov, N. A., and Eskes, H.: Enhanced Capabilities of TROPOMI NO₂: Estimating NO_x from North American Cities and Power Plants, *Environ Sci Technol*, 53, 12594–12601, <https://doi.org/10.1021/ACS.EST.9B04488>, 2019a.
Goldberg, D. L., Lu, Z., Oda, T., Lamsal, L. N., Liu, F., Griffin, D., McLinden, C. A., Krotkov, N. A., Duncan, B. N., and Streets, D. G.: Exploiting OMI NO₂ satellite observations to infer fossil-fuel CO₂ emissions from U.S.
420 megacities, *Science of The Total Environment*, 695, 133805, <https://doi.org/10.1016/J.SCITOTENV.2019.133805>, 2019b.
Goldberg, D. L., Anenberg, S. C., Kerr, G. H., Moheg, A., Lu, Z., and Streets, D. G.: TROPOMI NO₂ in the United States: A Detailed Look at the Annual Averages, Weekly Cycles, Effects of Temperature, and Correlation With Surface NO₂ Concentrations, *Earths Future*, 9, e2020EF001665, <https://doi.org/10.1029/2020EF001665>, 2021.
- 425 Goldberg, D. L., Tao, M., Kerr, G. H., Ma, S., Tong, D. Q., Fiore, A. M., Dickens, A. F., Adelman, Z. E., and Anenberg, S. C.: Evaluating the spatial patterns of U.S. urban NO_x emissions using TROPOMI NO₂, *Remote Sens Environ*, 300, 113917, <https://doi.org/10.1016/J.RSE.2023.113917>, 2024.
Gonzalez Abad, G., Souri, A. H., Bak, J., Chance, K., Flynn, L. E., Krotkov, N. A., Lamsal, L., Li, C., Liu, X., Miller, C. C., Nowlan, C. R., Suleiman, R., and Wang, H.: Five decades observing Earth’s atmospheric trace gases
430 using ultraviolet and visible backscatter solar radiation from space, *J Quant Spectrosc Radiat Transf*, 238, 106478, <https://doi.org/10.1016/J.JQSRT.2019.04.030>, 2019.
Griffis, T. J., Lee, X., Baker, J. M., Russelle, M. P., Zhang, X., Venterea, R., and Millet, D. B.: Reconciling the differences between top-down and bottom-up estimates of nitrous oxide emissions for the U.S. Corn Belt, *Global Biogeochem Cycles*, 27, 746–754, <https://doi.org/10.1002/GBC.20066>, 2013.
- 435 Gvakharia, A., Kort, E. A., Brandt, A., Peischl, J., Ryerson, T. B., Schwarz, J. P., Smith, M. L., and Sweeney, C.: Methane, Black Carbon, and Ethane Emissions from Natural Gas Flares in the Bakken Shale, North Dakota, *Environ Sci Technol*, 51, 5317–5325, <https://doi.org/10.1021/ACS.EST.6B05183>, 2017.



- Gvakharia, A., Kort, E. A., Smith, M. L., and Conley, S.: Evaluating Cropland N₂O Emissions and Fertilizer Plant Greenhouse Gas Emissions With Airborne Observations, *Journal of Geophysical Research: Atmospheres*, 125, e2020JD032815, <https://doi.org/10.1029/2020JD032815>, 2020.
- Harrison, R. M., Yamulki, S., Goulding, K. W. T., and Webster, C. P.: Effect of fertilizer application on NO and N₂O fluxes from agricultural fields, *J Geophys Res*, 100, 25923–25931, <https://doi.org/10.1029/95JD02461>, 1995.
- Herrera, S. A., Diskin, G. S., Harward, C., Sachse, G., De Wekker, S. F. J., Yang, M., Choi, Y., Wisthaler, A., Mallia, D. V., and Pusede, S. E.: Wintertime Nitrous Oxide Emissions in the San Joaquin Valley of California Estimated from Aircraft Observations, *Environ Sci Technol*, 55, 4462–4473, <https://doi.org/10.1021/ACS.EST.0C08418>, 2021.
- Huber, D. E., Steiner, A. L., and Kort, E. A.: Daily Cropland Soil NO_x Emissions Identified by TROPOMI and SMAP, *Geophys Res Lett*, 47, e2020GL089949, <https://doi.org/10.1029/2020GL089949>, 2020.
- Huber, D. E., Kort, E. A., and Steiner, A. L.: Soil Moisture, Soil NO_x and Regional Air Quality in the Agricultural Central United States, *Journal of Geophysical Research: Atmospheres*, 129, e2024JD041015, <https://doi.org/10.1029/2024JD041015>, 2024.
- Ialongo, I., Virta, H., Eskes, H., Hovila, J., and Douros, J.: Comparison of TROPOMI/Sentinel-5 Precursor NO₂ observations with ground-based measurements in Helsinki, *Atmos Meas Tech*, 13, 205–218, <https://doi.org/10.5194/AMT-13-205-2020>, 2020.
- Jacob, D. J.: Introduction to Atmospheric Chemistry, *Introduction to Atmospheric Chemistry*, 1–280, 1999.
- Jaeglé, L., Martin, R. V., Chance, K., Steinberger, L., Kurosu, T. P., Jacob, D. J., Modi, A. I., Yoboué, V., Sigha-Nkamdjou, L., and Galy-Lacaux, C.: Satellite mapping of rain-induced nitric oxide emissions from soils, *Journal of Geophysical Research: Atmospheres*, 109, 21310, <https://doi.org/10.1029/2004JD004787>, 2004.
- Jimenez, R., Herndon, S., Shorter, J. H., Nelson, D. D., McManus, J. B., and Zahniser, M. S.: Atmospheric trace gas measurements using a dual quantum-cascade laser mid-infrared absorption spectrometer, <https://doi.org/10.1117/12.597130>, 2005.
- Johansson, C.: Field measurements of emission of nitric oxide from fertilized and unfertilized forest soils in Sweden, *J Atmos Chem*, 1, 429–442, <https://doi.org/10.1007/BF00053804>, 1984.
- Johansson, C. and Sanhueza, E.: Emission of NO from savanna soils during rainy season, *Journal of Geophysical Research: Atmospheres*, 93, 14193–14198, <https://doi.org/10.1029/JD093ID11P14193>, 1988.
- Kim, D. G., Vargas, R., Bond-Lamberty, B., and Turetsky, M. R.: Effects of soil rewetting and thawing on soil gas fluxes: A review of current literature and suggestions for future research, *Biogeosciences*, 9, 2459–2483, <https://doi.org/10.5194/BG-9-2459-2012>, 2012.
- Kort, E. A., Eluszkiewicz, J., Stephens, B. B., Miller, J. B., Gerbig, C., Nehrkorn, T., Daube, B. C., Kaplan, J. O., Houweling, S., and Wofsy, S. C.: Emissions of CH₄ and N₂O over the United States and Canada based on a receptor-oriented modeling framework and COBRA-NA atmospheric observations, *Geophys Res Lett*, 35, <https://doi.org/10.1029/2008GL034031>, 2008.
- Kort, E. A., Patra, P. K., Ishijima, K., Daube, B. C., Jiménez, R., Elkins, J., Hurst, D., Moore, F. L., Sweeney, C., and Wofsy, S. C.: Tropospheric distribution and variability of N₂O: Evidence for strong tropical emissions, *Geophys Res Lett*, 38, <https://doi.org/10.1029/2011GL047612>, 2011.
- Kort, E. A., Plant, G., Dacic, N. *Aircraft Data (2021) for Measurement of Agriculture Illuminating farm-Zone Emissions of N₂O (MAIZE)*, University of Michigan - Deep Blue Data. <https://doi.org/10.7302/0jvh-0c91>, 2022
- Kort, E. A., Plant, G., Dacic, N. *Aircraft Data (2022) for Measurement of Agriculture Illuminating farm-Zone Emissions of N₂O (MAIZE)*, University of Michigan - Deep Blue Data. <https://doi.org/10.7302/tmfd-nw87>, 2024



- 480 Kort, E. A., Plant, G., Dacic, N. *Posterior Flux Ensemble for Measurement of Agriculture Illuminating farm-Zone Emissions of N₂O (MAIZE)*, University of Michigan - Deep Blue Data. <https://doi.org/10.7302/9w5m-mn30>, 2024
- Lawrence, N. C., Tenesaca, C. G., VanLoocke, A., and Hall, S. J.: Nitrous oxide emissions from agricultural soils challenge climate sustainability in the US Corn Belt, *Proc Natl Acad Sci U S A*, 118, e2112108118, <https://doi.org/10.1073/PNAS.2112108118>, 2021.
- 485 Levine, J. S., Winstead, E. L., Parsons, D. A. B., Scholes, M. C., Scholes, R. J., Cofer, W. R., Cahoon, D. R., and Sebach, D. I.: Biogenic soil emissions of nitric oxide (NO) and nitrous oxide (N₂O) from savannas in South Africa: The impact of wetting and burning, *Journal of Geophysical Research: Atmospheres*, 101, 23689–23697, <https://doi.org/10.1029/96JD01661>, 1996.
- 490 Liang, Q., Nevison, C., Dlugokencky, E., Hall, B. D., and Dutton, G.: 3-D Atmospheric Modeling of the Global Budget of N₂O and Its Isotopologues for 1980–2019: The Impact of Anthropogenic Emissions, *Global Biogeochem Cycles*, 36, e2021GB007202, <https://doi.org/10.1029/2021GB007202>, 2022.
- Lin, X., van der A, R. J., de Laat, J., Huijnen, V., Mijling, B., Ding, J., Eskes, H., Douros, J., Liu, M., Zhang, X., Liu, Z., van der, R. A., and Liu avander, Z.: European soil NO_x emissions derived from satellite NO₂ observations, *Authorea Preprints*, <https://doi.org/10.22541/ESSOAR.170224578.81570487/V1>, 2023.
- 495 Lipschultz, F., Zafiriou, O. C., Wofsy, S. C., McElroy, M. B., Valois, F. W., and Watson, S. W.: Production of NO and N₂O by soil nitrifying bacteria, *Nature*, 294, 641–643, <https://doi.org/10.1038/294641A0>, 1981.
- Liu, S., Lin, F., Wu, S., Ji, C., Sun, Y., Jin, Y., Li, S., Li, Z., and Zou, J.: A meta-analysis of fertilizer-induced soil NO and combined NO+N₂O emissions, *Glob Chang Biol*, 23, 2520–2532, <https://doi.org/10.1111/GCB.13485>, 2017.
- 500 di Marco, C., Skiba, U., Weston, K., Hargreaves, K., and Fowler, D.: Field scale N₂O flux measurements from grassland using eddy covariance, *Water, Air, & Soil Pollution: Focus* 2004 4:6, 4, 143–149, <https://doi.org/10.1007/S11267-005-3024-X>, 2005.
- Merlos, F. A. and Hijmans, R. J.: The scale dependency of spatial crop species diversity and its relation to temporal diversity, *Proc Natl Acad Sci U S A*, 117, 26176–26182, <https://doi.org/10.1073/PNAS.2011702117>, 2020.
- 505 Müller, C., Kammann, C., Ottow, J. C. G., and Jäger, H. J.: Nitrous oxide emission from frozen grassland soil and during thawing periods, *Journal of Plant Nutrition and Soil Science*, 166, 46–53, <https://doi.org/10.1002/JPLN.200390011>, 2003.
- Nevison, C., Andrews, A., Thoning, K., Dlugokencky, E., Sweeney, C., Miller, S., Saikawa, E., Benmergui, J., Fischer, M., Mountain, M., and Nehrkorn, T.: Nitrous Oxide Emissions Estimated With the CarbonTracker-Lagrange North American Regional Inversion Framework, *Global Biogeochem Cycles*, 32, 463–485, <https://doi.org/10.1002/2017GB005759>, 2018.
- 510 Nevison, C., Lan, X., and Ogle, S. M.: Remote Sensing Soil Freeze-Thaw Status and North American N₂O Emissions From a Regional Inversion, *Global Biogeochem Cycles*, 37, e2023GB007759, <https://doi.org/10.1029/2023GB007759>, 2023.
- 515 Oikawa, P. Y., Ge, C., Wang, J., Eberwein, J. R., Liang, L. L., Allsman, L. A., Grantz, D. A., and Jenerette, G. D.: Unusually high soil nitrogen oxide emissions influence air quality in a high-temperature agricultural region, *Nat Commun*, 6, 1–10, <https://doi.org/10.1038/NCOMMS9753>, 2015.
- Park, J. U., Park, J. S., Diaz, D. S., Gebetsberger, M., Müller, M., Shalaby, L., Tiefengraber, M., Kim, H. J., Park, S. S., Song, C. K., and Kim, S. W.: Spatiotemporal inhomogeneity of total column NO₂ in a polluted urban area inferred from TROPOMI and Pandora intercomparisons, *GIsci Remote Sens*, 59, 354–373, <https://doi.org/10.1080/15481603.2022.2026640>, 2022.
- 520



- Pollack, I. B., Lerner, B. M., and Ryerson, T. B.: Evaluation of ultraviolet light-emitting diodes for detection of atmospheric NO₂ by photolysis - Chemiluminescence, *J Atmos Chem*, 65, 111–125, <https://doi.org/10.1007/S10874-011-9184-3>, 2010.
- 525 Ravishankara, A. R., Daniel, J. S., and Portmann, R. W.: Nitrous oxide (N₂O): The dominant ozone-depleting substance emitted in the 21st century, *Science* (1979), 326, 123–125, <https://doi.org/10.1126/SCIENCE.1176985>, 2009.
- Rowlings, D. W., Grace, P. R., Scheer, C., and Liu, S.: Rainfall variability drives interannual variation in N₂O emissions from a humid, subtropical pasture, *Science of The Total Environment*, 512–513, 8–18, <https://doi.org/10.1016/J.SCITOTENV.2015.01.011>, 2015.
- 530 Ryerson, T. B., Huey, L. G., Knapp, K., Neuman, J. A., Parrish, D. D., Sueper, D. T., and Fehsenfeld, F. C.: Design and initial characterization of an inlet for gas-phase NO_y measurements from aircraft, *Journal of Geophysical Research: Atmospheres*, 104, 5483–5492, <https://doi.org/10.1029/1998JD100087>, 1999.
- 535 Ryerson, T. B., Trainer, M., Holloway, J. S., Parrish, D. D., Huey, L. G., Sueper, D. T., Frost, G. J., Donnelly, S. G., Schauffler, S., Atlas, E. L., Kuster, W. C., Goldan, P. D., Hübler, G., Meagher, J. F., and Fehsenfeld, F. C.: Observations of ozone formation in power plant plumes and implications for ozone control strategies, *Science* (1979), 292, 719–723, <https://doi.org/10.1126/SCIENCE.1058113>, 2001.
- 540 Ryerson, T. B., Trainer, M., Angevine, W. M., Brock, C. A., Dissly, R. W., Fehsenfeld, F. C., Frost, G. J., Goldan, P. D., Holloway, J. S., Hübler, G., Jakoubek, R. O., Kuster, W. C., Neuman, J. A., Nicks, D. K., Parrish, D. D., Roberts, J. M., Sueper, D. T., Atlas, E. L., Donnelly, S. G., Flocke, F., Fried, A., Potter, W. T., Schauffler, S., Stroud, V., Weinheimer, A. J., Wert, B. P., Wiedinmyer, C., Alvarez, R. J., Banta, R. M., Darby, L. S., and Senff, C. J.: Effect of petrochemical industrial emissions of reactive alkenes and NO_x on tropospheric ozone formation in Houston, Texas, *Journal of Geophysical Research: Atmospheres*, 108, 4249, <https://doi.org/10.1029/2002JD003070>, 2003.
- 545 Sanhueza, E., Wei Min Hao, Scharffe, D., Donoso, L., and Crutzen, P. J.: N₂O and NO emissions from soils of the northern part of the Guayana Shield, Venezuela, *J Geophys Res*, 95, 22481–22488, <https://doi.org/10.1029/JD095ID13P22481>, 1990.
- Scholes, M. C., Martin, R., Scholes, R. J., Parsons, D., and Winstead, E.: NO and N₂O emissions from savanna soils following the first simulated rains of the season, *Nutr Cycl Agroecosyst*, 48, 115–122, <https://doi.org/10.1023/A:1009781420199>, 1997.
- 550 Shepherd, M. F., Barzetti, S., and Hastie, D. R.: The production of atmospheric NO_x and N₂O from a fertilized agricultural soil, *Atmospheric Environment. Part A. General Topics*, 25, 1961–1969, [https://doi.org/10.1016/0960-1686\(91\)90277-E](https://doi.org/10.1016/0960-1686(91)90277-E), 1991.
- 555 Sihi, D., Davidson, E. A., Savage, K. E., and Liang, D.: Simultaneous numerical representation of soil microsite production and consumption of carbon dioxide, methane, and nitrous oxide using probability distribution functions, *Glob Chang Biol*, 26, 200–218, <https://doi.org/10.1111/GCB.14855>, 2020.
- Skiba, U., Smith, K. A., and fowler, D.: Nitrification and denitrification as sources of nitric oxide and nitrous oxide in a sandy loam soil, *Soil Biol Biochem*, 25, 1527–1536, [https://doi.org/10.1016/0038-0717\(93\)90007-X](https://doi.org/10.1016/0038-0717(93)90007-X), 1993.
- 560 Smith, K. A., McTaggart, I. P., and Tsuruta, H.: Emissions of N₂O and NO associated with nitrogen fertilization in intensive agriculture, and the potential for mitigation, *Soil Use Manag*, 13, 296–304, <https://doi.org/10.1111/J.1475-2743.1997.TB00601.X>, 1997.
- Strum, M., Eyth, A., and Vukovich, J.: Preparation of Emissions Inventories for the Version 7, 2014 Emissions Modeling Platform for NATA, 2017.



- 565 Tian, H., Xu, R., Canadell, J. G., Thompson, R. L., Winiwarter, W., Suntharalingam, P., Davidson, E. A., Ciais, P., Jackson, R. B., Janssens-Maenhout, G., Prather, M. J., Regnier, P., Pan, N., Pan, S., Peters, G. P., Shi, H., Tubiello, F. N., Zaehle, S., Zhou, F., Arneeth, A., Battaglia, G., Berthet, S., Bopp, L., Bouwman, A. F., Buitenhuis, E. T., Chang, J., Chipperfield, M. P., Dangal, S. R. S., Dlugokencky, E., Elkins, J. W., Eyre, B. D., Fu, B., Hall, B., Ito, A., Joos, F., Krummel, P. B., Landolfi, A., Laruelle, G. G., Lauerwald, R., Li, W., Lienert, S., Maavara, T., MacLeod, M., Millet, D. B., Olin, S., Patra, P. K., Prinn, R. G., Raymond, P. A., Ruiz, D. J., van der Werf, G. R., Vuichard, N.,
570 Wang, J., Weiss, R. F., Wells, K. C., Wilson, C., Yang, J., and Yao, Y.: A comprehensive quantification of global nitrous oxide sources and sinks, *Nature*, 586, 248–256, <https://doi.org/10.1038/S41586-020-2780-0>, 2020.
- 575 Tian, H., Pan, N., Thompson, R. L., Canadell, J. G., Suntharalingam, P., Regnier, P., Davidson, E. A., Prather, M., Ciais, P., Muntean, M., Pan, S., Winiwarter, W., Zaehle, S., Zhou, F., Jackson, R. B., Bange, H. W., Berthet, S., Bian, Z., Bianchi, D., Bouwman, A. F., Buitenhuis, E. T., Dutton, G., Hu, M., Ito, A., Jain, A. K., Jeltsch-Thömmes, A., Joos, F., Kou-Giesbrecht, S., Krummel, P. B., Lan, X., Landolfi, A., Lauerwald, R., Li, Y., Lu, C., Maavara, T., Manizza, M., Millet, D. B., Mühle, J., Patra, P. K., Peters, G. P., Qin, X., Raymond, P., Resplandy, L., Rosentreter, J. A., Shi, H., Sun, Q., Tonina, D., Tubiello, F. N., Van Der Werf, G. R., Vuichard, N., Wang, J., Wells, K. C., Western, L. M., Wilson, C., Yang, J., Yao, Y., You, Y., and Zhu, Q.: Global nitrous oxide budget (1980–2020), *Earth Syst Sci Data*, 16, 2543–2604, <https://doi.org/10.5194/ESSD-16-2543-2024>, 2024.
- 580 Tortoso, A. C. and Hutchinson, G. L.: Contributions of autotrophic and heterotrophic nitrifiers to soil NO and N₂O emissions, *Appl Environ Microbiol*, 56, 1799–1805, <https://doi.org/10.1128/AEM.56.6.1799-1805.1990>, 1990.
- 585 Xiang, B., Miller, S. M., Kort, E. A., Santoni, G. W., Daube, B. C., Commane, R., Angevine, W. M., Ryerson, T. B., Trainer, M. K., Andrews, A. E., Nehrkorn, T., Tian, H., and Wofsy, S. C.: Nitrous oxide (N₂O) emissions from California based on 2010 CalNex airborne measurements, *Journal of Geophysical Research: Atmospheres*, 118, 2809–2820, <https://doi.org/10.1002/JGRD.50189>, 2013.
- Yang, R., Hayashi, K., Zhu, B., Li, F., and Yan, X.: Atmospheric NH₃ and NO₂ concentration and nitrogen deposition in an agricultural catchment of Eastern China, *Science of The Total Environment*, 408, 4624–4632, <https://doi.org/10.1016/J.SCITOTENV.2010.06.006>, 2010.
- 590 Zannetti, P., Van, Reinhold, N., and York, N.: Air Pollution Modeling Theories, Computational Methods, Computational Mechanics Publications Southampton Boston, 2013